

# OVER 10% EFFICIENT SCREEN PRINTED RGS SOLAR CELLS

Giso Hahn<sup>1</sup>, Sven Seren<sup>1</sup>, Detlef Sontag<sup>1</sup>,  
Astrid Gutjahr<sup>2</sup>, Leon Laas<sup>2</sup>, Axel Schönecker<sup>2</sup>

<sup>1</sup> University of Konstanz, Department of Physics, 78457 Konstanz, Germany

<sup>2</sup> ECN - Energy Research Centre of the Netherlands, P.O. Box 1, 1755 LE Petten, Netherlands

## ABSTRACT

The ribbon-growth-on-substrate (RGS) technology has the potential to produce wafers for PV at low cost and high speed without silicon losses related to wafer cutting. Up to now a discontinuously operating R&D machine produces test wafers with high oxygen content. Special care had therefore to be taken to prevent the formation of recombination centres related to oxygen formed at high temperatures during cell processing. Solar cells fabricated from RGS material with high oxygen content using an evaporation process resulted in efficiencies of up to 12.8%. An industrial-type screen printing process led to efficiencies of up to 10.5%. To further increase efficiency, the oxygen content has to be reduced. After a rebuilding of the RGS machine wafers reveal significantly lower oxygen contents. First screen printed cells made from that material show higher currents and open circuit voltages but not yet higher efficiencies due to shunting problems caused by current collecting structures.

## 1. INTRODUCTION

In the last years a remarkable growth of the PV industry with annual growth rates well above 25% was achieved. It is expected that PV can and will maintain growth rates in the 25 to 35% range in the foreseeable future. This also means that the PV industry has to adjust its manufacturing capacities to satisfy the market.

Thus technological developments can be expected in all parts of the PV module production chain, from solar grade silicon, over wafer and solar cell manufacturing to module production. In the field of wafer production, the ribbon-growth-on-substrate silicon wafer technology promises the effective production of silicon wafers at low manufacturing costs, at high production rate and with almost 100% silicon usage.

### The RGS technology

The ribbon-growth-on-substrate technology is a silicon wafer manufacturing technology, which belongs to the class of high speed ribbon technologies, where crystallization is de-coupled from wafer production speed (see principle of the RGS technology in Fig. 1).

This technology was developed by Bayer AG [1] throughout the 80's and 90's. Since 2000 a Dutch consortium of ECN and S'Energy is developing the RGS technology further with the objective to commercialize it in 2005 [2].

## 2. DISCONTINUOUS MACHINE

The principle of the RGS wafer casting process is simple. A substrate plate with a temperature below silicon melting point is moved underneath a casting frame filled with liquid silicon. The silicon is forced to crystallize on the colder substrates due to extraction of the heat [3]. Crystal growth direction and ribbon production direction are perpendicular to each other. The crystallized Si ribbon leaves the casting frame on top of the substrate and detaches during cooling down.

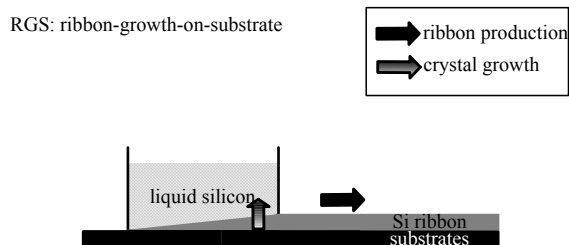


Fig. 1: Principle of the RGS ribbon growth process.

In the original process from Bayer the Si material is molten in a quartz glass crucible at high temperature. During melting  $\text{SiO}_2$  is dissolved in the liquid silicon. In consequence the content of oxygen [O] in the cast wafers is comparably high ( $2 \times 10^{18} \text{ cm}^{-3}$ ). The extremely high oxygen concentration in RGS wafers caused all sort of oxygen clusters, precipitation as well as new or thermal donors to be present in the wafers. Thus thermal processing strategies had to be developed, which allowed the use of high oxygen containing RGS wafers for solar cells.

In the past two strategies were applied. Large oxygen precipitates can be formed in an annealing step at temperatures above 1000 °C directly after crystallization. These precipitates are electrically less active and are principally stable during the cell processing steps.

The second option is to rapidly cool down the cast wafer after crystallization and keep the oxygen dissolved on interstitial sites in the Si lattice. This material reacts to a 'normal' solar cell process with the formation of new donors, which prohibit its use in a standard process. Rapid thermal processing in combination with the avoidance of the critical temperature ranges was applied successfully on RGS wafers [4].

### 3. REDUCING [O<sub>i</sub>]

As the high oxygen content of  $2 \times 10^{18} \text{ cm}^{-3}$  forms a major obstacle for the use of RGS wafers, the existing RGS machine was rebuilt in order to allow for different refractory materials and lower melting temperatures. Experiments using pure graphite or coated environments at different temperatures were performed. After casting all wafers were rapidly cooled down to keep the oxygen in its interstitial form and to minimize the formation of oxygen precipitates. FTIR spectrometry was used to analyze the interstitial oxygen content [O<sub>i</sub>] in the wafers. The results listed in Table I show, that the concentration of [O<sub>i</sub>] could be lowered by a factor of two compared to material produced earlier.

**Table I:** Interstitial oxygen concentration in RGS wafers. Wafers cast from Si molten in different environments and temperatures.

Si molten	low temperature		high temperature	
	Exp.	[O <sub>i</sub> ] (10 <sup>17</sup> at/cm <sup>3</sup> )	Exp.	[O <sub>i</sub> ] (10 <sup>17</sup> at/cm <sup>3</sup> )
in graphite	157	6-10	158	9-11
	159	7-10	160	7-10
with coating	161	6-9	162	6-8
	164	6-10	165	5-8

An additional smaller source for oxygen is introduced by the process gas during the casting process. This can be concluded from the increasing values for [O<sub>i</sub>] from the first to the last wafer during a single run (Fig. 2). Better gas management during the experiment should be the key to keep the oxygen level on a constant low value, because [O<sub>i</sub>] for wafers in the beginning of the process is already comparable to standard cast multi-crystalline material.

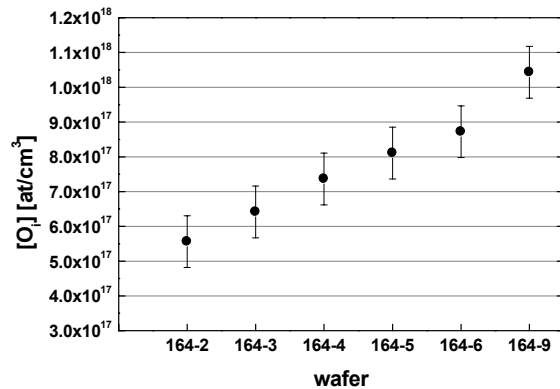


**Fig. 2:** Interstitial oxygen content [O<sub>i</sub>] in RGS wafers successively cast in a single run.

### 4. SOLAR CELL PROCESSING

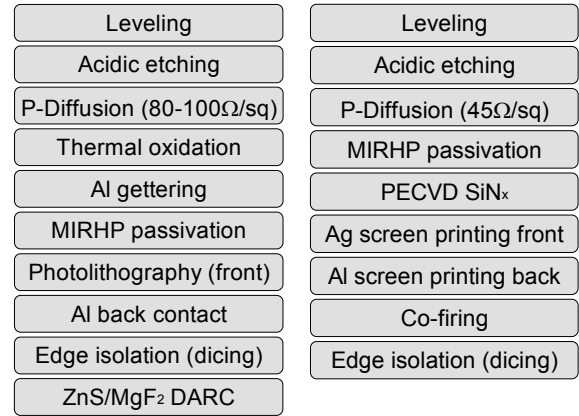


**Fig. 3:** Evaporation process used for determination of potential in efficiency for RGS material (left), and screen printing process used for industrial-type processing (right).

#### 4.1 Evaporation Process

The potential in efficiency of RGS material can be best investigated by applying a simple and reliable process. In our investigation we have chosen a process based on evaporation of metal contacts and photolithography for front grid formation as shown in Fig. 3 (left).

After leveling of the uneven front surface using a conventional dicing saw with a planarisation tool mounted on the spindle, the saw damage is removed by acidic etching, followed by a POCl<sub>3</sub>-diffusion and thermal oxidation for passivating the front surface. Following evaporation of 2 μm Al, a gettering step for 30 min at 800 °C removes metallic impurities. A microwave-induced remote hydrogen plasma (MIRHP) passivation step is carried out for bulk passivation [5]. Both front (photolithography, Ti/Pd/Ag) and back contact (Al) are formed by electron beam evaporation. Finally, the 5x5 cm<sup>2</sup> wafers are diced into 2x2 cm<sup>2</sup> solar cells.

Investigations using this process have been carried out with high [O] material, which underwent an annealing step directly after crystallization as described in section 3. Table II gives cell parameters of the best RGS cell fabricated according to this process. It is known from other experiments [5] that a macroscopic V-texture of the RGS wafer surface can increase efficiency further (up to 8%<sub>rel</sub>).

**Table II:** Cell parameters of the best 4 cm<sup>2</sup> RGS cell fabricated according to the evaporation process shown in Fig. 3, left (independently confirmed at EC JRC Ispra).

	V <sub>oc</sub> [mV]	J <sub>sc</sub> [mA/cm <sup>2</sup> ]	FF [%]	η [%]
best RGS solar cell	575	28.6	78.1	12.8

The map of the effective diffusion length (L<sub>eff</sub>) obtained by spatially resolved IQE and reflectivity measurements presented in Fig. 4 reveals that despite of an optimized MIRHP step for bulk passivation, crystal defects are still limiting cell efficiency. Therefore we conclude that significantly higher efficiencies can only be obtained for RGS material if [O] can be lowered.

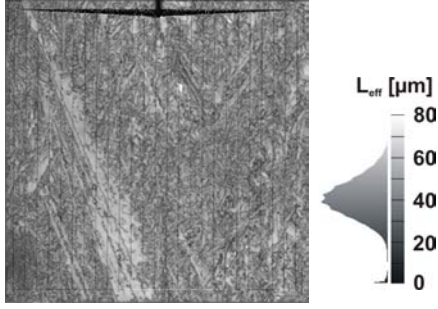


**Fig. 4:**  $L_{\text{eff}}$  map of the best  $2 \times 2 \text{ cm}^2$  RGS solar cell.

#### 4.2. Industrial-type processing

Besides the potential of the RGS material tested in the evaporation process in section 4.1, we were interested in the performance of RGS material in an industrial-type state-of-the-art cell process. A screen printing fire through SiN process was chosen, as can be seen from Fig. 3 (right). A PECVD SiN<sub>x</sub> layer is deposited in a direct plasma reactor using low frequency, which serves both as an antireflective coating as well as a reservoir of hydrogen to be released into the bulk during the high temperature co-firing step for passivating defects and contact formation. Former experiments revealed that hydrogen diffusion is slowed down in materials with high [O<sub>i</sub>] [5], therefore an additional MIRHP passivation step was implemented.

The advantage of the industrial-type processing is a higher throughput. This process is less time consuming than the evaporation process, but due to the limited quantity of RGS wafers in the current R&D phase and the larger area of the cells ( $5 \times 5 \text{ cm}^2$ ), experiments have to be planned more carefully. Nevertheless, results after a change in crystallization parameters can be obtained more quickly, therefore all experiments concerning reduction of [O] have been performed with the screen printing process up to now.

##### 4.2.1 High [O<sub>i</sub>]

Before the rebuilding of the RGS machine for reducing [O<sub>i</sub>] as described in section 3, solar cells have been processed according to Fig. 3 (right) with material including the same annealing step as applied for the best cell in section 4.1. IV parameters of one of the best cells are given in Table III. Another cell showed an efficiency of 10.5%.

The lower  $J_{\text{sc}}$  values as compared to Table II can be explained by a higher grid shadowing, more reflectivity (only SiN<sub>x</sub> as single layer ARC), and a less effective hydrogen passivation because of out-diffusion of hydrogen during the PECVD SiN<sub>x</sub> deposition. The lower  $V_{\text{oc}}$  might be caused by the less effective hydrogen passivation and the poorer surface passivation.

A  $L_{\text{eff}}$  map of this cell is presented in Fig. 5. As compared to Fig. 4, a slight drop of  $L_{\text{eff}}$  can be detected which can be ascribed to the less effective hydrogenation.

**Table III:** IV data of one of the best screen printed RGS solar cells ( $5 \times 5 \text{ cm}^2$ ) before rebuilding of the RGS machine in order to reduce [O<sub>i</sub>].

	$V_{\text{oc}}$ [mV]	$J_{\text{sc}}$ [mA/cm <sup>2</sup> ]	FF [%]	$\eta$ [%]
$5 \times 5 \text{ cm}^2$ RGS cell	565	24.2	76.3	10.4

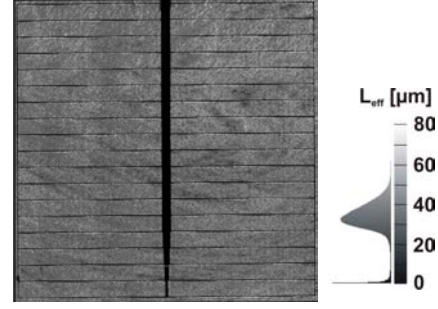


**Fig. 5:**  $L_{\text{eff}}$  map of the screen printed  $5 \times 5 \text{ cm}^2$  RGS solar cell from Table III. Less effective hydrogenation leads to lower  $L_{\text{eff}}$  values as compared to Fig. 4.

##### 4.2.2 Reduced [O<sub>i</sub>]

As described in section 3, a rebuilding of parts in the RGS machine led to lower [O<sub>i</sub>]. According to [5] this should result in faster hydrogenation leading to higher  $L_{\text{eff}}$  and an increased  $J_{\text{sc}}$ . The material with reduced [O<sub>i</sub>] was fabricated without an annealing step after crystallization. Cells have been processed from wafers with lower [O<sub>i</sub>] as measured by FTIR (Table I). Although  $J_{\text{sc}}$  could be increased for some cells as can be seen in Fig. 6 and  $V_{\text{oc}}$  of up to 573 mV could be obtained, cell efficiency decreased because of very poor fill factors. Fits to the dark IV curves revealed that a poor shunt resistance  $R_{\text{sh}}$  is the cause for the drop in FF (Fig. 7).

The reason for the shunting maybe SiC formation. Thermography can locate areas with shunting activity (Fig. 8, left). These areas match very well with unusually high values in internal quantum efficiency (IQE, Fig. 8, middle). The IQE signal at shunting locations is most probably caused by current collecting channels [5], which are known to exist in RGS material. Up to now they were related to oxygen precipitates forming an inversion layer around the precipitates, but now we have first evidence that they might be caused by SiC as well, as [O] is significantly reduced in these wafers. Bulk lifetimes  $\tau_{\text{b}}$  are lower or average in these regions, proving that the unusually high IQE signal is not related to large diffusion lengths but to another current collection mechanism (Fig. 8, right). Lifetimes could be increased to  $2 \mu\text{s}$  in the low [O<sub>i</sub>] material, explaining the higher  $J_{\text{sc}}$  and  $V_{\text{oc}}$ .

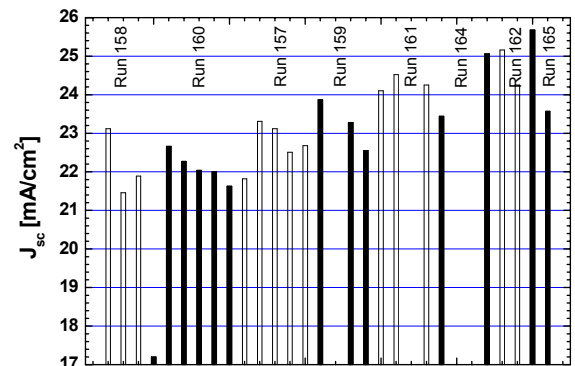


**Fig. 6:**  $J_{\text{sc}}$  for RGS solar cells with a reduced [O<sub>i</sub>]. RGS material was fabricated without annealing step after crystallization.

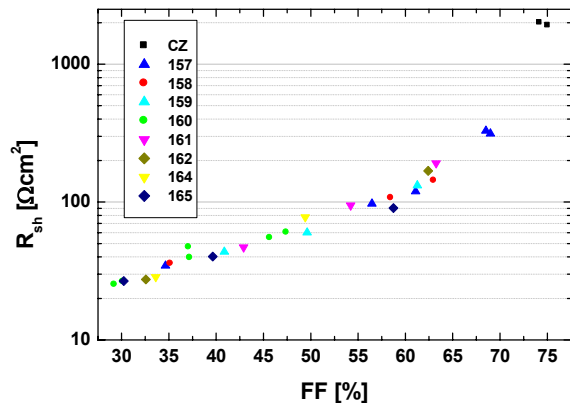


Fig. 7: Poor  $R_{sh}$  in RGS cells is the cause for low FF and resulting lower efficiencies despite of a reduced  $[O_i]$  as compared to the cell presented in section 4.1.

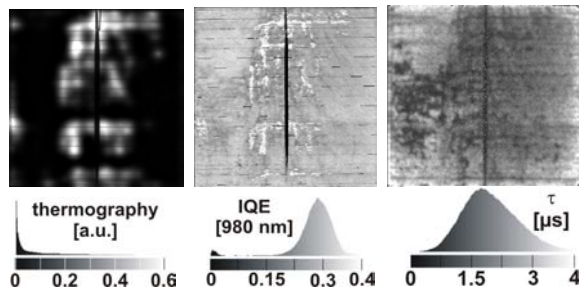


Fig. 8: Thermography (left) and IQE (middle) of a  $5 \times 5 \text{ cm}^2$  RGS solar cell with reduced  $[O_i]$ . Shunts can be visualized by their thermal activity and match well with a higher IQE. Lifetimes (right) could be increased to  $2 \mu\text{s}$ .

In summary, we can state that the reduction of  $[O_i]$  in the RGS fabrication process allows to omit the high temperature annealing step due to the strongly decreased formation of recombination active new donors during subsequent high temperature steps in the cell process. A better hydrogenation allows higher lifetimes of up to  $2 \mu\text{s}$  in this material, resulting in an increased  $J_{sc}$  and  $V_{oc}$ . If the shunting problem can be avoided, the reduction of  $[O]$  should result in significantly higher efficiencies. The reduction of carbon concentration will therefore be the next step to improve cell efficiencies further.

## 5. OUTLOOK RGS TECHNOLOGY

In order to successfully commercialize the RGS technology, two major challenges have to be met. On one side the wafer quality should allow for sufficiently high solar cell efficiencies in standard solar cell processes. Reducing the oxygen content is the first step in that direction. Carbon concentration, dislocation density and crystal structure will follow.

On the other side the development of a reliable continuously operating RGS casting machine must be worked out in parallel. Due to its high productivity of 24 million wafers per year, machine up time, maintenance intervals and reliability of ware parts are most critical. As

final stage of the machine design phase, these questions are worked out.

## 6. CONCLUSION

The high speed wafer growth of the RGS technology offers good prospect for a significant cost reduction in PV. Solar cells with efficiencies of up to 12.8% (evaporation process) and 10.5% (screen printing) could be processed. The high oxygen content, known as a limiting factor in RGS cells, was significantly reduced after a rebuilding of the discontinuously operating R&D machine for RGS wafer fabrication. First screen printed solar cells were processed out of this material. For the first time it was possible to process RGS wafers without oxygen annealing step in a screen-printing process. Compared to former annealed, high oxygen RGS material, the best solar cells reached higher short-circuit currents and open circuit voltages because of higher carrier lifetimes. However, an efficiency increase could not yet been observed due to very poor fill factors caused by a shunting mechanism, which is most probably caused by SiC formation due to the high carbon content of the material. Avoiding these shunts should increase efficiencies further.

## 7. ACKNOWLEDGEMENTS

We gratefully acknowledge the support from the Dutch Economy, Ecology and Technology program (E.E.T.) under contract number EETK99150 and of the EC under contract number ENK6-CT2001-00574.

## REFERENCES

- [1] W. Koch, H.-U. Höfs, C. Häßler and S. Thurm, "Preparation, characterisation and cell processing of Bayer RGS silicon foils (Ribbon Growth on Substrate)", *Proc. 2<sup>nd</sup> WC PVSEC*, Vienna 1998, 1254
- [2] A. Schönecker, L. Laas, A. Gutjahr, P. Wyers, A. Reinink and B. Wiersma, "Ribbon-Growth-on-Substrate: Progress in high speed crystalline silicon wafer manufacturing", *Proc. 29<sup>th</sup> IEEE PVSC*, New Orleans 2002, 316
- [3] A. Schönecker, L. Laas, A. Gutjahr, M. Goris, P. Wyers, G. Hahn and D. Sontag, "Ribbon-Growth-on-Substrate: Challenges and promises of high speed silicon wafer manufacturing", *12<sup>th</sup> NREL workshop on silicon solar cell materials*, Breckenridge 2002, 7 ([www.osti.gov/bridge](http://www.osti.gov/bridge))
- [4] S. Peters, C. Ballif, D. Borchert, V. Radt, R. Schindler, W. Warta, G. Willeke, C. Häßler and T. Lauinger, "Improving the efficiency of silicon ribbon solar cells using rapid thermal processing", *Proc. 17<sup>th</sup> EC PVSEC*, Munich 2001, 1319
- [5] G. Hahn, C. Haessler and M. Langenkamp, "12.5% efficient RGS solar cells with carrier collecting channels", *Proc. 17<sup>th</sup> EC PVSEC*, Munich 2001, 1371